*Journal of Mathematics and Informatics*
*Vol. 21, 2021, 53-64*
*ISSN: 2349-0632 (P), 2349-0640 (online)*
*Published 22 November 2021*
*www.researchmathsci.org*
*DOI: http://dx.doi.org/10.22457/jmi.v21a05198*

Journal of
Mathematics and Informatics

# Image Fusion Based on NSST and CSR Under Robust Principal Component Analysis

***Li Quanjun*[1*]，*Zhang Guicang*[1] and *Han Genliang*[2]**

[1]School of Mathematics and Statistics, Northwest Normal University
Lanzhou,730070, China.
[2]Key Laboratory of Sensors and Sensing Technology
Lanzhou, 730070, China
[*]Corresponding author. E-mail: 15248193664@163.com

*Received 6 September 2021; accepted 13 October 2021*

***Abstract.*** Aiming at the problems of loss of detail information and noise interference that are easy to produce in the image fusion process, a robust principal component analysis (RPCA) based on Convolutional Sparse Coding (CSR) and For image fusion of Non-Subsampled Shear Wave Transform (NSST), the source image is pre-enhanced first; then the image is decomposed by RPCA to obtain low-rank images and sparse images; then NSST fusion is used respectively For low-rank images, CSR coding is used to fuse sparse images, and finally two separately fused images are synthesized to obtain the final fused image. Experimental results show that the algorithm in this paper can effectively improve the contrast and clarity of the fused image, reduce noise interference, rich scene information, clear targets, and overall objective evaluation indicators are better than existing algorithms, and the operating efficiency has also been improved

***Keywords:*** Robust principal component analysis; non-subsampled shear wave transform; convolutional sparse coding

***AMS Mathematics Subject Classification (2010):*** 62H35

## 1. Introduction

Based on the difference of the sensor that acquires the image, its imaging principle and working environment will produce complementary and redundant information due to different images. Graphic fusion is to synthesize different information of the same scene into an image through a specific algorithm, overcome the limitations and differences of a

single sensor image, and obtain a more comprehensive and accurate description of the scene. Infrared image is imaged by the thermal radiation of the object itself, because it is difficult to detect the non-heating target, which will make the image details and textures not rich, and the contrast will be small. Visible light images are imaged by the reflection of visible light. Such imaging makes texture details and contrast more suitable for human eye observation. Therefore, the contrast of the two images is different and needs to be adjusted before fusion.

In recent years, image fusion technology has developed rapidly, and many fusion methods have been proposed. From the framework of analysis, it can be divided into image fusion methods based on deep learning, based on transform domain, and based on sparse representation. Image fusion methods based on deep learning generally require a large amount of prior knowledge based on multi-scale transformation, but it is difficult to obtain prior knowledge, and it is very difficult to obtain a large amount of prior knowledge, which limits the application of such methods. Multi-scale transformation has been widely used in the field of image fusion, and the choice of transformation method and fusion rule after decomposition is an extremely important issue. Commonly used for image fusion are pyramid transform (NSPF), Laplace transform (LP), curvelet transform (CVT) and the transform used in this article (NSST). NSST transformation is to use NSPF to decompose the image multiple times. Since downsampling is not used, the image has translation invariance during image fusion. The reconstructed image can avoid the pseudo-Gibbs phenomenon and has high operating efficiency, but lacks the expression of details, resulting in scene information. Slightly worse, so it can't be used alone, and better results can be obtained when used in conjunction with other methods. The method based on sparse representation is to reconstruct the image according to the over-complete dictionary in the spatial domain, and use the sliding window technology to block the source image, so as to obtain the image information more effectively. The dictionary can be obtained through traditional analytical formulas or after training.The approach will cause damage to some structure and feature information of the image, thereby affecting the entire structural feature. The image fusion method based on convolutional sparse coding can process the whole image, and has the characteristic of not being restricted by the image dimension, so it can obtain richer texture detail information for image information and features.

To solve the above problems, this paper proposes an image fusion method based on NSST and CSR under RPCA. First, the function is used to adjust the contrast of the two source images to make it more suitable for image fusion; the RPCA method decomposes the image matrix into low rank Matrix and sparse matrix, low-rank matrix and sparse

matrix respectively represent different information. In the image matrix, the salient information of the source image can be described by the features extracted from the sparse matrix. In the infrared image, the target is the prominent information and the prominent part that is different from the blurred background. Therefore, infrared target information can be modeled as a component related to a sparse matrix, and background information can be modeled as a component related to a low-rank matrix. At the same time, the NSST and CSR fusion methods are used to make full use of the advantages of the two to process the images separately, and different fusion rules are used to fuse the low-rank part and the sparse part respectively. This can make full use of the advantages of the two to process the images separately, and finally reconstruct the fusion image

## 2. Related background knowledge

### 2.1. Robust principal component analysis

RPCA assumes an image matrix, and what classical PCA studies is to find a low-rank matrix that minimizes the difference between and. The classic assumes that the data is Gaussian, but in actual applications, once there is a large noise and serious outliers or large measured data, it will have a great impact on PCA, resulting in failure to give ideal results. Like PCA, RPCA is essentially the problem of finding the best projection of data in low-dimensional space. The proposal of RPCA improves this defect of PCA. It can recover low-rank data from large and sparse noise-polluted observation data. In short, the core idea of RPCA is that the data matrix can be expressed as a superposition of a low-rank matrix and a sparse matrix under the optimization criterion. which is:

$$A = L + S \tag{1}$$

where and L are S unknown.

Under the optimal criterion, RPCA can be written as the following optimization problem: Under the optimal criterion, RPCA can be written as the following optimization problem:

$$\min_{L,S}\{rank(L) + \lambda \|S\|_0\} \qquad s.t. A = L + S \tag{2}$$

Among them, $rank(L)$ represents the rank of the matrix L and $\|S\|_0$ represents the number of non-zeros of the matrix S.

However, $rank(L)$ and $L_0$ norms have non-convex and non-smooth characteristics in optimization, so this NP-hard problem is generally converted to solve a relaxed convex optimization problem:

$$\min_{L,S}\{\|L\|_* + \lambda\|S\|_1\} \qquad s.t. A = L + S \tag{3}$$

Among them, $\|L\|_*$ is the nuclear norm of $L$. $\|S\|_1$ is the $L_1$ norm of $S$, and $\lambda$ is the balance parameter.

## 2.2. Non-subsampled shear wave transform

Shear wave transform is a novel multi-scale geometric analysis tool, but its discretization process is usually realized by down-sampling, so it is not translation invariant. Easley et al. used two steps of multi-scale decomposition and direction localization to perform the discretization process. In this way, the standard shear filter was mapped from the pseudo-polarization grid system back to the Cartesian coordinate system, and the down-sampling operation was cleverly discarded to achieve the effect of translation invariance.

In fact, it is also a synthetic wavelet used, and its formula is:

$$D_{MN}(\psi) = \left\{\psi_{j,l,k}(x) = |\det M|^{j/2}\psi\left(N^l M^j - K\right),\ j,l \in Z, K \in Z^2\right\} \tag{4}$$

In the formula, $\psi \in L^2\left(R^2\right)$, $|\det N| = 1$, $j$ is the decomposition scale, $l$ is the direction parameter, $k$ is the shearing parameter; $M$ is the anisotropic matrix, $N$ is the shearing matrix, and $Z$ is the integer domain. When:

$$M = M_0 = \begin{bmatrix} 4 & 0 \\ 0 & 2 \end{bmatrix}, N = N_0 = \begin{bmatrix} 1 & 1 \\ 0 & 1 \end{bmatrix} \tag{5}$$

When this is a special case of synthetic wavelet, it is the NSST algorithm used in this article. Figure 1 is a schematic diagram of the two-level decomposition of NSST. The two-level decomposition is similar, where SPF is a shear wave filter.

## 2.3. Convolutional sparse coding

In sparse representation theory, two major problems must be solved first and foremost: the construction of an over-complete dictionary and the sparse coefficient decomposition

algorithm. For an image matrix Y, given a dictionary $D=[d_1,d_2,\ldots,d_n]$, the image Y can be expressed as:

$$Y=\sum_{i=1}^{n} d_i x_i = DX \tag{6}$$

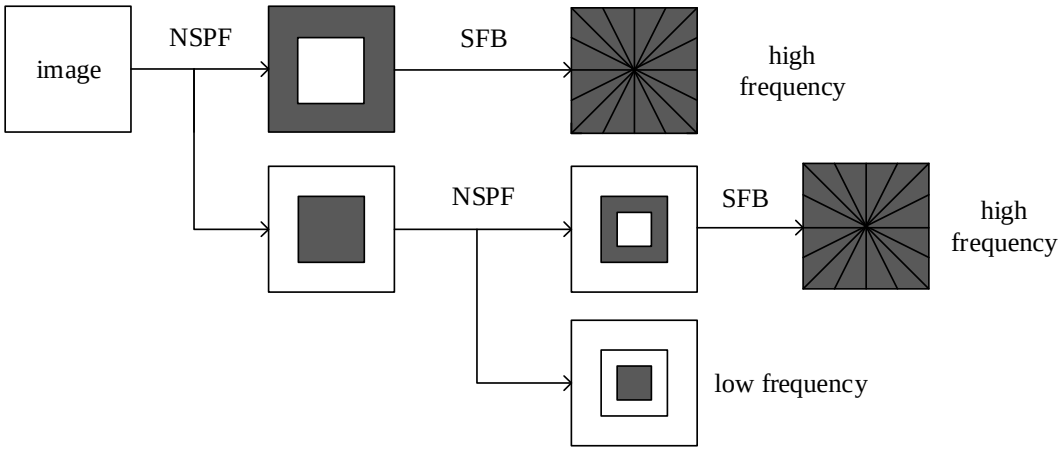


**Figure 1:** Schematic diagram of the two-level decomposition of NSST

Among them, $X=[x_1,x_2,\ldots,x_n]$ is the corresponding coefficient represented by the dictionary D on the image Y. When Y and D is determined, X can be solved by the following formula:

$$x=\arg\min_{x}\frac{1}{2}\|Dx-Y\|_2^2+\lambda\|x\|_1 \tag{7}$$

If the product in the formula is replaced by convolution, this is the convolution sparse coding proposed by Zeiler et al., then the above formula becomes

$$x_m=\arg\min_{x_m}\left\{\frac{1}{2}\left\|\sum_m d_m\otimes x_m-Y\right\|_F^2+\lambda\|x_m\|_1\right\} \tag{8}$$

Table $\otimes$ is convolution, $\{d_m\}$ is M-dimensional convolution dictionary, $\{x_m\}$ is convolution sparse coefficient, $\lambda$ is balance parameter, and this formula can be solved by ADMM algorithm, then the formula can be transformed into:

$$\{d_m,x_m\}=\arg\min_{x_m}\left\{\frac{1}{2}\left\|\sum_{m=1}^{M} d_m\otimes x_m\right\|_F^2+\lambda\sum_{m=1}^{M}\|x_m\|_1\right\} \qquad s.t.\|d_m\|_2=1 \tag{9}$$

## 3. The method of this article

### 3.1. Image preprocessing

Because the sensor is affected by its own characteristics and the shooting environment, the contrast of the captured image is relatively small. In order to better present texture information and scene clarity, it is imperative to improve image contrast. This paper uses the following T function to enlarge the pixels larger than $\mu$ in the image and reduce the pixels smaller than $\mu$, which is defined as:

$$\mathrm{T}(x,y)=\frac{255}{k_l \exp(-(10S(x,y)/255-5))+1} \tag{10}$$

$$k_l=\frac{255/\mu-1}{\exp[-(10\mu/255-5)]} \tag{11}$$

Among them, $S(x,y)$ is the pixel gray value of the image at $(x,y)$; $\mu$ is the average pixel value of the image; $T(x,y)$ is the gray value of the pixel at $(x,y)$ after contrast stretching; $k_l$ is the inflection point parameter. Infrared source image A and visible light source image B are preprocessed infrared image $A_1$ and visible light image $B_1$ to obtain low-rank parts $L_1$ and $L_2$ and sparse parts $S_1$ and $S_2$ after RPCA decomposition.

### 3.2. NSST fusion rule

The low-rank parts $L_1$ and $L_2$ are decomposed into low-frequency parts $L_{1l}$ and $L_{2l}$ and high-frequency parts $L_{1h}$ and $L_{2h}$ after NSST transformation. Since the main feature information of the image is mostly resolved to the sparse part, the low-rank part is mostly the contour and background of the image, etc. The main energy such as letter, so the low-frequency part of this article uses weighted average, which is:

$$L_l=0.5L_{1l}+0.5L_{2l} \tag{12}$$

In the high frequency part, the visible light has richer texture details, so a slight deviation of the proportion will produce better results, namely:

$$L_l=0.4L_{1h}+0.6L_{2h} \tag{13}$$

### 3.3. CSR fusion rule

The sparse parts $S_1$ and $S_2$ decomposed by RPCA are decomposed by convolution to obtain the corresponding convolution coefficients $X_1$ and $X_2$, and then the absolute values of the corresponding positions of all elements of $X_1$ and $X_2$ are calculated as the sum of $Y_1$ and $Y_2$, which is:

$$Y_k(i,j)=\sum_{t=1}^{n}\left|X_k(i,j,t)\right| \tag{14}$$

where $k = 1, 2$, and then use the imfilter function to perform convolution filtering on $Y_1$ and $Y_2$ to obtain matrices $Y_1^{'}$ and $Y_2^{'}$, where the filtering matrix K is:

$$K = \frac{1}{49} ones(7,7) \tag{15}$$

Finally, compare the elements in $Y_1^{'}$ and $Y_2^{'}$ and take the big rules to get the fused filtered matrix Z, and then inversely get the fused image matrix of sparse components, namely:

$$Z(i, j) = \max\{Y_1^{'}(i, j), Y_2^{'}(i, j)\} \tag{16}$$

### 3.4. Algorithm flow chart of the proposed method

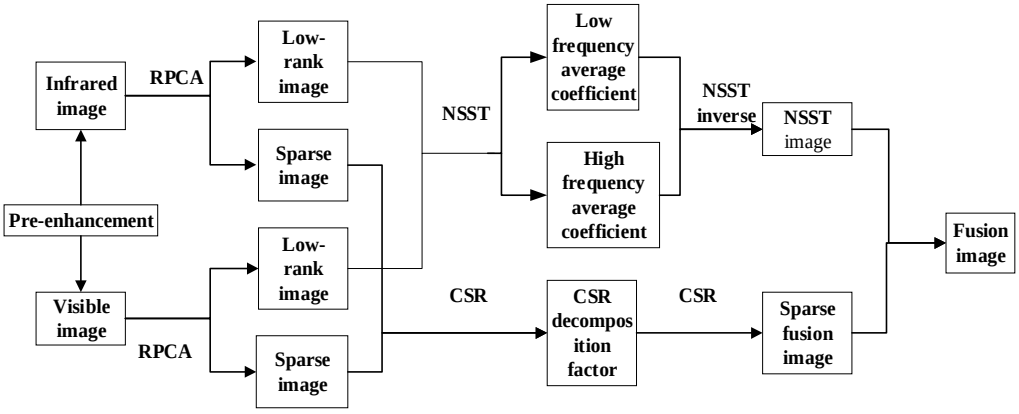


**Figure 2:** Flow chart of the proposed method

### Algorithm

**Step 1:** Perform RPCA decomposition on the source image after pre-enhancement processing;

**Step 2:** Perform NSST decomposition on the low-rank image, and then the coefficients are weighted and averaged respectively, and the low-rank image is obtained by inverse transformation;

**Step 3:** After CSR decomposition of the sparse image, the absolute value of the coefficient is taken as large as the fusion coefficient, and the image is reconstructed;

**Step 4:** Add the low-rank image and the sparse image to get the final fused image.

## 4. Experimental results and analysis

In order to verify the effectiveness of the algorithm (RNC) in this paper, two sets of strictly registered infrared images and visible light images are selected for fusion, and the size of

all images is $256\times256$, as shown in Figure 1. The algorithm in this paper is experimentally compared with the existing fusion algorithms. The five algorithms are based on NSST, CSR, SR, LPT, and WTF image fusion algorithms. In the algorithm of this article, the inflection point parameters of the pre-enhancement processing $k_l = 3$, the RPCA error $tol = 10^{-15}$, the maximum number of iterations $\max\_iter = 15000$, the key CSR parameters, the experimental operating environment is Matlab2019a, the processor Intel(R) Core(TM) i5-5200U CPU@2.20GH 2.20GHz, windows10 .

The effect of image fusion can be divided into supervisory visual evaluation and objective performance evaluation. Subjective refers to the personal subjective evaluation of the target information and texture details of the image through the human eye, while objective evaluation refers to the measurement of the fusion effect of the image through a specific function , This article mainly evaluates the fusion image objectively from six aspects: information entropy (IE), average gradient (AG), spatial frequency (SF), standard deviation (SD), image definition (G), edge strength (Q), etc. , The larger the above index value, the better the effect. The first is the fusion effect of the first picture as follows:

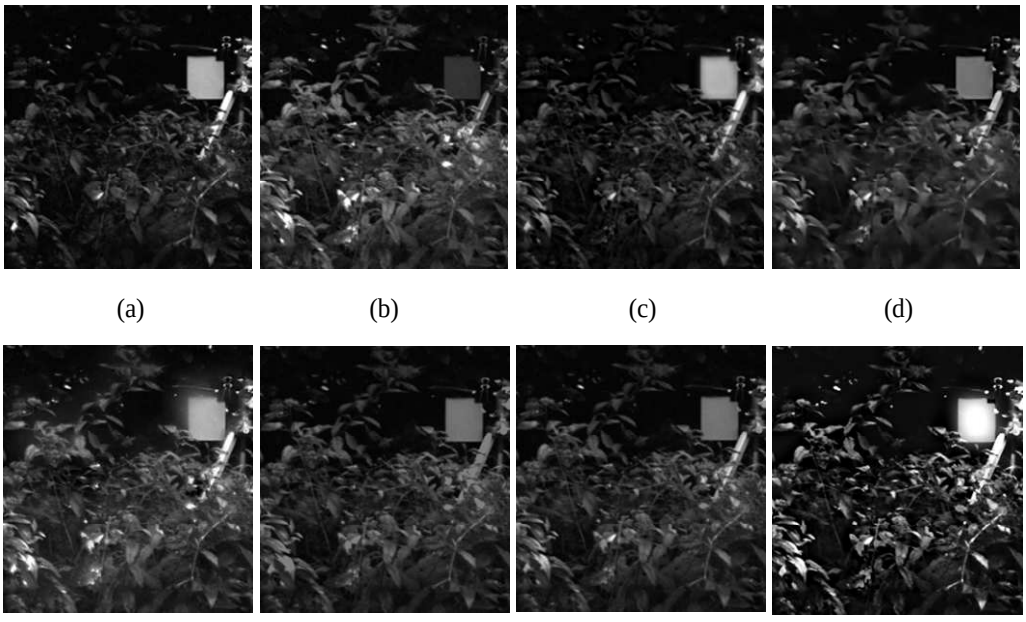

(a) (b) (c) (d)

**Figure 3:** Flower cluster fusion image (a) Visible light image (b) Infrared image (c) NSST (d) CSR (e) LPT (f) SR (g) WTF (h) proposed method

**Figure 4:** Objective evaluation index of flower cluster fusion image

| Method | RNC | NSST | CSR | WTF | SR | LPT |
|---|---|---|---|---|---|---|
| IE | 6.4804 | 6.1958 | 6.4244 | 6.3927 | 6.3031 | 6.9206 |
| AG | 10.7185 | 5.8352 | 5.5416 | 6.1168 | 5.8557 | 7.2623 |
| SF | 31.9816 | 14.3646 | 15.9308 | 15.5007 | 14.5871 | 19.3588 |
| SD | 53.9955 | 34.9143 | 32.0965 | 31.3332 | 29.5972 | 40.3826 |
| G | 12.543 | 6.5168 | 6.1557 | 7.0732 | 6.7837 | 8.6739 |
| Q | 109.9025 | 61.1008 | 58.6973 | 63.2357 | 60.5388 | 74.1986 |

From the perspective of the image fusion effect, (c)-(h) in Figure 3 have achieved the fusion effect, but from a subjective point of view (c)(d)(f) and (g) are rich in details, but The target is not obvious. (e) Although the target is obvious, the image is obviously blurred. The algorithm in this paper can better present the detailed texture information, and the clear target information is convenient for subsequent image analysis. From the analysis of objective indicators in Figure 4, the algorithm in this paper is significantly better than other algorithms, especially G and Q, except that the IE value is slightly lower than that of the LPT algorithm. That is, regardless of the subjective or objective effect, the method in this paper is generally the best.

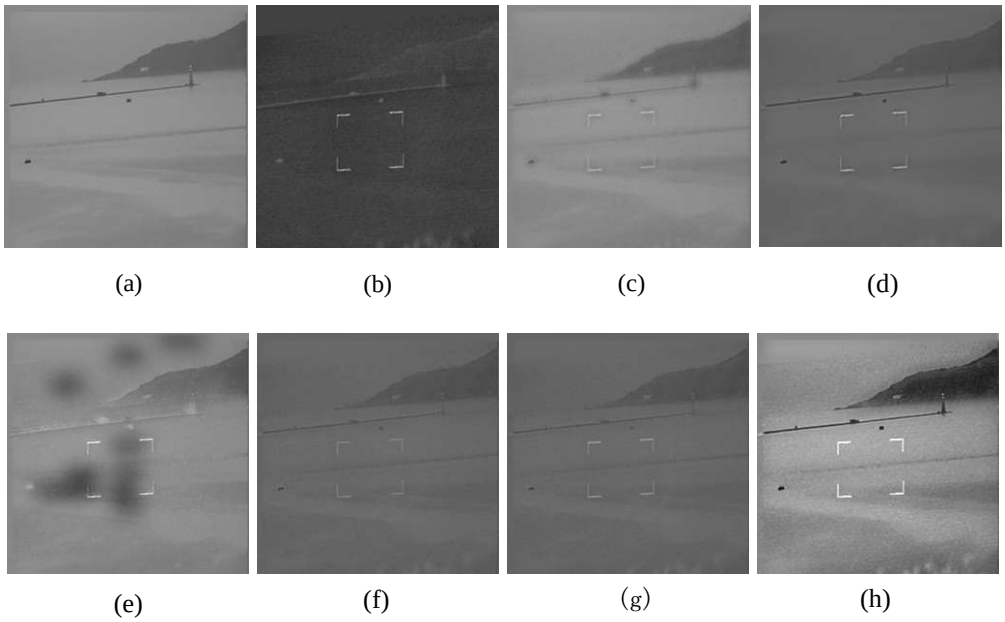


**Figure 5:** Beach fusion image (a) Visible light image (b) Infrared image (c) NSST (d) CSR (e) LPT (f) SR (g) WTF (h) proposed method

**Figure 6:** Objective evaluation index of beach fusion image

| Method | R+N+C | NSST | CSR | WTF | SR | LPT |
|---|---|---|---|---|---|---|
| IE | 6.3592 | 5.0783 | 4.1657 | 4.3170 | 4.3104 | 5.533909 |
| AG | 3.8962 | 1.2510 | 0.6683 | 1.3262 | 1.3035 | 1.828098 |
| SF | 12.8917 | 3.4137 | 4.5523 | 4.1453 | 3.7699 | 6.670372 |
| SD | 27.7324 | 12.1827 | 6.7165 | 6.4215 | 6.2439 | 14.403519 |
| G | 5.6561 | 1.5894 | 0.7859 | 1.9430 | 1.9109 | 2.636387 |
| Q | 35.5043 | 12.2241 | 6.9588 | 11.9478 | 11.7070 | 16.686465 |

From a subjective point of view, the image in Figure 5 achieves a fusion effect in all methods except (e). (c) The image is blurred, and the target and background information are very fuzzy and difficult to identify. The image targets of (f) and (g) are dim, difficult to locate, with dark background and low definition. (d) Although the effect is good, the overall effect is still very bleak, which is far from the algorithm of this paper. The fusion method in this paper has clear objectives, sufficient brightness and obvious outline, which is very convenient for subsequent image analysis. For the objectively listed indexes in Figure 6, the algorithm in this paper is superior to other algorithms, and it is much higher than other algorithms in SD, G, and Q indexes, which proves that the algorithm in this paper is the optimal algorithm.

## 5. Conclusion

In order to solve the problems of low definition, low target recognition, and loss of detailed texture information that may occur in the fusion of infrared and visible images, this paper proposes an image fusion method based on NSST and CSR under robust principal component analysis. This method can effectively solve the above problems, and is superior to other algorithms in subjective and objective indicators. However, the research based on robust principal component analysis still needs further research, and the algorithm complexity in this paper still needs to be further optimized. Therefore, there are many aspects of the method in this paper that need to be improved.

***Acknowledgements:*** National Natural Science Foundation of China (61861040), Gansu Academy of Sciences Applied Research and Development (2018JK-02), Gansu Province Key Research and Development Program (20YF8GA125), Gansu Province Key Laboratory of Sensors and Sensing Technology Open Fund Project (KF-6), Lanzhou Municipal Science and Technology Plan Project (2018-4-35), Northwest Normal

University 2020 Graduate Research Funding Project (2020KYZZ001127), Gansu Province Excellent Graduate Student "Innovation Star" Project (2021CXZX-266).

We also thankful to the reviewers for pointing out some issues for betterment of the paper.

**Conflict of interest.** The authors declare that they have no conflict of interest.

**Authors' Contributions.** All the authors contribute equally to this work.

## REFERENCES

1. Huang Xiaosheng and Xu Jing, Non-subsampled shear wave domain multi-focus image fusion based on PCANet, *Computer Science*, 48(9) (2021) 181-186.
2. Wang Lifang, Dou Jieliang, Qin Pinle, Lin Suzhen, Gao Yuan and Zhang Chengcheng, Medical image fusion combining dual dictionary learning and adaptive PCNN, *Chinese Journal of Image and Graphics*, 24(9) (2019) 1588-1603.
3. Qiu Jiale, Research on image convolution sparse representation algorithm, *Nanjing University of Posts and Telecommunications*, 2020.
4. Li Yu, Shi Na, Kong Huihua and Lei Xiaoxue, Sparse angle CT reconstruction algorithm based on full variation and gradient domain convolution sparse coding, *Progress in Laser and Optoelectronics*, 58(12) (2021) 339 -348.
5. Rajat C.Shinde, Surya S.Durbha and Abhishek V.Potnis, LidarCSNet: A deep convolutional compressive sensing reconstruction framework for 3D airborne lidar point cloud, *ISPRS Journal of Photogrammetry and Remote Sensing*, 180 (2021) 313-334.
6. Zhang Lei, Zhang Yu, Ma Shibang and Yang Fengbao, CT and MRI image fusion algorithm based on hybrid [formula omitted] layer decomposing and two-dimensional variation transform, *Biomedical Signal Processing and Control*, 70 (2021) 103024.
7. Gao Yuan, Ma Shiwei, Liu Jingjing, Liu Yanyan, Zhang Xianxia, Fusion of medical images based on salient features extraction by PSO optimized fuzzy logic in NSST domain, *Biomedical Signal Processing and Control*, 69 (2021) 102852.
8. Li Liangliang, Ma Hongbing, Saliency-Guided Nonsubsampled Shearlet transform for multisource remote sensing image fusion, Sensors (Basel, Switzerland), 2021, 21(5) 1756-1769.
9. D. Satyanarayana, K. Vanitha and M.N.G. Prasad, Multi-modal medical image fusion algorithm based on spatial frequency motivated PA-PCNN in the NSST domain, *Current Medical Imaging*, 17(5) (2021) 634-643.

10. Feng Shanshan, Lin Yun, Wang Yanping, Teng Fei and Hong Wen, 3D point cloud reconstruction using inversely mapping and voting from single pass CSAR images, *Remote Sensing*, 13(17) (2021) 3534-3534.
11. Liu Jingjing, Xiu Xianchao, Jiang Xin, Liu Wanquan, Zeng Xiaoyang, Wang Mingyu and Chen Hui, Manifold constrained joint sparse learning via non-convex regularization, *Neur ocomputing*, 458 (2021) 112-126.
12. Talbi Hassiba, Kholladi Mohamed Khireddine, DEPSO With DTCWT algorithm for multimodal medical image fusion, *International Journal of Applied Metaheuristic Computing*, 12(4) (2021) 78-97.
13. Huang Chenjian and Dai Wenzhan, Combining UDWT and PCNN medical image fusion algorithm in NSST domain, *Optoelectronics· Laser*, 31(11) (2020) 1157-1165.
14. Jiang Zhaozhen, Han Yusheng, Xie Ruichao and Ren Shuaijun, Research on an infrared polarization image fusion algorithm based on NSST transform, *Optoelectronics Laser*, 31(11) (2020) 1140-1148.
15. Wang Zhao, Du Qingzhi, Dong Anyong, Su Bin and Zhao Wenbo, Infrared and visible light image fusion based on non-subsampled shear wave transform, *Optoelectronics· Laser*, 31(10) (2020) 1062-1073.